Tris(2,2′-bipyridine)ruthenium(II) Cations as Photoprobes of Clay Tactoid Architecture within Hectorite and Laponite Films

Michael E. Hagerman,* Samuel J. Salamone, Robert W. Herbst, and Amy L. Payeur

Department of Chemistry, Union College, Schenectady, New York 12308

Received September 16, 2002. Revised Manuscript Received November 12, 2002

The adsorption and intercalation of the cationic luminescence probe, tris(2,2′-bipyridine)-ruthenium(II) complex ($[Ru(bpy)_3]^{2+}$ or Rubpy), into hectorite and Laponite host clay films were investigated. Because the photophysical properties of Rubpy are strongly influenced by the lamellar nanospace of the smectite host, Rubpy serves as a unique photoprobe of host−guest and guest−guest interfaces within inorganic−organic nanocomposites. The stacking patterns of the host tactoids influence guest luminescence through direct mediation of ion clustering and self-quenching phenomena. Spectral red shift of emission wavelengths and decreased lifetimes were observed with increased guest loading. The extent of red shift in the Rubpy/Laponite films indicated a more fluid guest microenvironment. Rubpy/Laponite films exhibit enhanced potential for photonic and sensor applications with increased optical transparency, intense luminescence, and longer luminescence lifetimes. Cointercalation of the cationic surfactant, trimethylcetylammonium cation, promotes two-dimensional tiling of Laponite tactoids and may afford selective tuning of fluorophore packing.

Introduction

Owing to their enhanced chemical stability and highly applicable photophysical and electrochemical properties,[1] tris(2,2′bipyridine)ruthenium(II) (abbreviated as $[Ru(bpy)_3]^{2+}$ or Rubpy) and analogous ruthenium complexes have found widespread applications in oxygen[2−4] and glucose sensors,[5] electrochemiluminescent immunoassays[6] and DNA probe assays,[7] photooxidizers,[8] heterogeneous photocatalysts,[9−12] light emitting devices,[13−16] fiber optic imaging sensors,[17] and bioinorganic chips for metalloprotein synthesis.[18] The incorporation of ruthenium chelates within inorganic host assemblies has produced photofunctional intercalation compounds with advanced materials applications. More specifically, $[Ru(bpy)_3]^{2+}$ and related ruthenium derivatives have been adsorbed within numerous media including zeolites,[9,19−23] mesoporous silica,[24] sol−gel systems,[25] layered zirconium phosphates,[26−29] chalcogeno-phosphates,[30] niobates/titanates,[31] and layered sulfides[32] and silicates.[33−48]

* To whom correspondence should be addressed.

(1) Kalyanasundaram, K. *Photochemistry of Polypyridine and Porphyrin Complexes*; Academic Press: London, 1992.
(2) Baker, G. A.; Wenner, B. R.; Watkins, A. N.; Bright, F. V. *J. Sol-Gel Sci. Technol.* **2000**, *17*, 71−82.
(3) McMurray, H. N.; Douglas, P.; Csilla, B.; Garley, M. S. *J. Photochem. Photobiol. A* **1994**, *80*, 283−288.
(4) Carraway, E. R.; Demas, J. N.; DeGraff, B. A.; Bacon, J. R. *Anal. Chem.* **1991**, *63*, 337−342.
(5) Ohsaka, T.; Yamagishi, Y.; Oyama, N. *Bull. Chem. Soc. Jpn.* **1990**, *63*, 2646.
(6) Fiaccabrino, G. C.; Koudelka-Hep, M.; Hsueh, Y.-T.; Collins, S. D.; Smith, R. L. *Anal. Chem.* **1998**, *70*, 4157−4161.
(7) Xu, X.; Bard, A. J. *J. Am. Chem. Soc.* **1995**, *117*, 2627−2631.
(8) Li, C.; Hoffman, M. Z. *J. Phys. Chem. A* **2000**, *104*, 5998−6002.
(9) Pettit, T. L.; Fox, M. A. *J. Phys. Chem.* **1986**, *90*, 1353−1354.
(10) Taniguchi, T.; Fukasawa, Y.; Miyashita, T. *J. Phys. Chem. B* **1999**, *103*, 1920−1924.
(11) Shklover, V.; Ovchinnikov, Y. E.; Braginsky, L. S.; Zakeeruddin, S. M.; Grätzel, M. *Chem. Mater.* **1998**, *10*, 2533−2541.
(12) Torres, G. R.; Dupart, E.; Mingotaud, C.; Ravaine, S. *J. Phys. Chem. B* **2000**, *104*, 9487−9490.
(13) Gao, F. G.; Bard, A. J. *J. Am. Chem. Soc.* **2000**, *122*, 7426−7427.
(14) Collinson, M. M.; Novak, B.; Martin, S. A.; Taussig, J. S. *Anal. Chem.* **2000**, *72*, 2914−2918.
(15) Collinson, M. M.; Taussig, J.; Martin, S. A. *Chem. Mater.* **1999**, *11*, 2594−2599.
(16) Masui, H.; Murray, R. W. *Inorg. Chem.* **1997**, *36*, 5118−5126.
(17) Walt, D. R. *Acc. Chem. Res.* **1998**, *31*, 267−278.
(18) Alsfasser, R.; van Eldik, R. *Inorg. Chem.* **1996**, *35*, 628−636.
(19) De Wilde, W.; Peeters, G.; Lunsford, J. H. *J. Phys. Chem.* **1980**, *84*, 2306−2310.
(20) Lainé, P.; Lanz, M.; Calzaferri, G. *Inorg. Chem.* **1996**, *35*, 3514−3518.
(21) Maruszewki, K.; Kincaid, J. R. *Inorg. Chem.* **1995**, *34*, 2002−2006.
(22) Szulbinski, W. S.; Kincaid, J. R. *Inorg. Chem.* **1998**, *57*, 859−864.
(23) Turbeville, W.; Robins, D. S.; Dutta, P. K. *J. Phys. Chem.* **1992**, *96*, 5024−5029.
(24) Ogawa, M.; Nakamura, T.; Mori, J.; Kuroda, K. *J. Phys. Chem. B* **1999**, *104*, 8554−8556.
(25) Matsui, K.; Momose, F. *Chem. Mater.* **1997**, *9*, 2588−2591.
(26) Colón, J. L.; Yang, C.-Y.; Clearfield, A.; Martin, C. R. *J. Phys. Chem.* **1988**, *92*, 5777−5781.
(27) Colón, J. L.; Yang, C.-Y.; Clearfield, A.; Martin, C. R. *J. Phys. Chem.* **1990**, *94*, 874−882.
(28) Kumar, C. V.; Williams, Z. J. *J. Phys. Chem.* **1995**, *99*, 17632−17639.
(29) Vliers, D. P.; Collin, D.; Schoonheydt, R. A.; De Schryver, F. C. *Langmuir* **1986**, *2*, 165−169.
(30) Jakubiak, R.; Francis, A. H. *J. Phys. Chem.* **1996**, *100*, 362−367.
(31) Nakato, T.; Kusunoki, K.; Yoshizawa, K.; Kuroda, K.; Kaneko, M. *J. Phys. Chem.* **1995**, *99*, 17896−17905.
(32) Poizat, O.; Sourisseau, C. *J. Phys. Chem.* **1984**, *88*, 3007−3014.
(33) Ogawa, M.; Takizawa, Y. *J. Phys. Chem. B* **1999**, *103*, 5005−5009.
(34) Ogawa, M.; Tsujimura, M.; Kuroda, K. *Langmuir* **2000**, *16*, 4202−4206.

10.1021/cm0209160 CCC: $25.00 © 2003 American Chemical Society
Published on Web 12/20/2002

Because of their rich intercalation chemistry and ability to enhance the temporal and thermal stability of the included guest, layered smectites are intriguing hosts for the fabrication of organic−inorganic nanocomposites.[49−54] A review of the photofunctions of intercalation compounds that includes a well-constructed summary of research on $[Ru(bpy)_3]^{2+}$ adsorbed within clay hosts has been provided by Ogawa and Kuroda.[39] The photophysical properties of $[Ru(bpy)_3]^{2+}$ incorporated in layered smectites are influenced by both strong host−guest[48] and guest−guest interactions.[55] A primary emphasis in this area has been on photophysical investigation of increased quantum yields of luminescence when $[Ru(bpy)_3]^{2+}$ complexes and other Ru(II) chelates were adsorbed in colloidal clay suspensions.[36,37,55−57] Numerous studies of the self-quenching reactions of these complexes have been reported.[36,37,40,47,55]

While several studies discuss film fabrication,[40,43,45,56,58] clear delineation of optimal guest loading for practical device fabrication has not been fully described for many of these lamellar hosts. Molecular recognition in lamellar solids that employ thin film strategies offer facile routes to practical chemical technologies including chemical sensing, separations, catalysis, and photonics.[59] The development of solid-state luminescence optical sensors based on $[Ru(bpy)_3]^{2+}$ intercalation compounds relies upon the following: a better understanding of how to suppress strong guest−guest interactions; ion clustering and subsequent self-quenching phenomena; and facile routes to film fabrication.

We have reported previously that hectorite films promote the spontaneous polymerization of a variety of organic monomers including aniline[60,61] and methyl methacrylate.[62] In this paper, we establish synthetic parameters for the loading of $[Ru(bpy)_3]^{2+}$ guest species within Laponite host films for future photoprobe studies of these and related clay/polymer systems. Because the photophysical properties of Rubpy are strongly influenced by the lamellar nanospace of the smectite host, we illustrate herein that Rubpy also serves as a unique photoprobe of host tactoid (clay platelet or microcrystal) architecture. In the current study, we also examine the cointercalation of cationic surfactants to promote selective tuning of Rubpy/clay and Rubpy−Rupby interactions. Delineation of clay platelet stacking within the host film matrix coupled with synthetic routes to control tactoid architectures may afford new inorganic/organic nanocomposites with enhanced optical and chemical sensing capabilities.

Experimental Section

Materials. $Ru(bpy)_3Cl_2 \cdot 6H_2O$ was purchased from Aldrich Co. Sodium exchanged hectorite powder ($Na_{0.33}[Mg_{2.67}Li_{0.33}]Si_4O_{10}[OH]_2$) was obtained from RHEOX, Highstown, NJ, and was used without further purification. The approximate cation exchange capacity (CEC) reported for this material is 100 mequiv/100 g. Analysis of typical samples of RHEOX hectorite yield 0.2% Fe. Sodium exchanged Laponite powder (Laponite RD ($Na_{0.7}[Li_{0.3}Mg_{5.5}Si_8O_{20}(OH)_4]$)) was provided by Southern Clay Products, Gonzalez, TX. The approximate CEC for Laponite is 72 mequiv/100 g.

Preparation of Clay Host Films. Preparation of the metal cation exchanged hectorite films was carried out as indicated by Eastman and co-workers[61] with a few minor changes. The salt solutions used were 0.5 M $Zn(NO_3)_2$ and 0.5 M $CuSO_4$. Each exchange used 0.4 g of Na-hectorite powder for every 100 mL of salt solution. The powder and solution were allowed to stir for 1 week. After the exchange, the clay from the $CuSO_4$ solution was washed and centrifuged until the supernatant produced a negative test for SO_4^{2-} (i.e. addition of $BaCl_2$ yielded no precipitate). The clay from the $Zn(NO_3)_2$ solution was washed and centrifuged a minimum of five times. Films were then cast by allowing a suspension of the clay to dry either free-standing in a polystyrene weigh boat or on fused quartz substrates. In the case of the weigh boat, the resultant films could be removed, cut, and mounted on various supports. In the case of the fused quartz, the films were strongly bound to their substrates.

Organically modified Laponite (OML) was prepared by dissolving alkylammonium halide salts (surfactants) in a 50:50 mixture of ethanol and deionized H_2O. An appropriate amount of guest mixture was added to prepared Zn−Lap in order to attain the desired loading. Loadings are given as a percentage of the smectite's CEC. The mixture was stirred for 7−12 h at 50−70 °C. OML slurries were then centrifuged and washed extensively with a 50:50 ethanol and deionized water mixture until a $AgNO_3$ test confirmed the absence of halide anions. Films were then cast from aqueous suspension on quartz microscope slides.

Preparation of $[Ru(bpy)_3^{2+}]$/Clay Nanocomposites. The incorporation of $[Ru(bpy)_3]^{2+}$ into the interlayer space of the clay films was conducted through facile aqueous exchange. Air-dried films were fully immersed in deionized water and exposed to exact guest concentrations in order to obtain desired loadings (reported in either mmol of guest/100 g of host or

(35) Joshi, V.; Ghosh, P. K. *J. Am. Chem. Soc.* **1989**, *111*, 5604−5612.
(36) Schoonheydt, R. A.; De Pauw, P.; Vliers, D.; De Schryver, F. C. *J. Phys. Chem.* **1984**, *88*, 5113−5118.
(37) DellaGuardia, R. A.; Thomas, J. K. *J. Phys. Chem.* **1983**, *87*, 990−998.
(38) Xiang, Y.; Villemure, G.; Detellier, C. *Clays Clay Miner.* **1992**, *40*, 362−364.
(39) Ogawa, M.; Kuroda, K. *Chem. Rev.* **1995**, *95*, 399−438.
(40) Kuykendall, V. G.; Thomas, J. K. *J. Phys. Chem.* **1990**, *94*, 4224−4230.
(41) Kamat, P. V.; Gopidas, K. R.; Mukherjee, T.; Joshi, V.; Kotkar, K.; Pathak, V. S.; Ghosh, P. K. *J. Phys. Chem.* **1991**, *95*, 10009−10018.
(42) Adbo, S.; Canesson, P.; Cruz, M.; Fripiat, J. J.; Damme, H. V. *J. Phys. Chem.* **1981**, *85*, 797−809.
(43) Traynor, M. F.; Mortland, M. M.; Pinnavaia, T. J. *Clays Clay Miner.* **1978**, *26*, 318−326.
(44) Nakamura, T.; Thomas, J. K. *Langmuir* **1985**, *1*, 568−573.
(45) Kuykendall, V.; Thomas, J. K. *Langmuir* **1990**, *6*, 1350−1356.
(46) Joshi, V.; Kotkar, D.; Ghosh, P. K. *J. Am. Chem. Soc.* **1986**, *108*, 4650−4651.
(47) Awaluddin, A.; DeGuzman, R. N.; Kumar, C. V.; Suib, S. L.; Burkett, S. L.; Davis, M. E. *J. Phys. Chem.* **1995**, *99*, 9886−9892.
(48) Turro, N. J.; Kumar, C. V.; Grauer, Z.; Barton, J. K. *Langmuir* **1987**, *3*, 1056−1059.
(49) Giannelis, E. P. *Adv. Mater.* **1996**, *8*, 29.
(50) Pinnavaia, T. J. In *Materials Chemistry: An Emerging Discipline*; Interrante, L. V., Casper, L. A., Ellis, A. B., Eds.; American Chemical Society: Washington, DC, 1995; pp 283−300.
(51) Vaia, R. A.; Teukolsky, R. K.; Giannelis, E. P. *Chem. Mater.* **1994**, *6*, 1017−1022.
(52) Schöllhorn, R. *Chem. Mater.* **1996**, *8*, 1747−1757.
(53) Kleinfeld, E. R.; Ferguson, G. S. *Chem. Mater.* **1995**, *7*, 2327−2331.
(54) Carrado, K.; Xu, L. *Chem. Mater.* **1998**, *10*, 1440−1445.
(55) Ghosh, P. K.; Bard, A. J. *J. Phys. Chem.* **1984**, *88*, 5519−5526.
(56) Kuykendall, V. G.; Thomas, J. K. *Langmuir* **1990**, *6*, 1351−1355.
(57) Villemure, G.; Detellier, C.; Szabo, A. G. *Langmuir* **1991**, *7*, 1215−1221.
(58) Krenske, D.; Abdo, S.; Damme, H. V.; Cruz, M.; Fripiat, J. J. *J. Phys. Chem.* **1980**, *84*, 2447−2457.
(59) Mallouk, T. E.; Gavin, J. A. *Acc. Chem. Res.* **1998**, *31*, 209−217.
(60) Porter, T. L.; Thompson, D.; Bradley, M.; Eastman, M. P.; Hagerman, M. E.; Attuso, J. L.; Votava, A. E.; Bain, E. D. *J. Vac. Sci. Technol. A* **1997**, *15*, 500−504.
(61) Porter, T. L.; Eastman, M. E.; Zhang, D. Y.; Hagerman, M. E. *J. Phys. Chem. B* **1997**, *101*.
(62) Salvador, P. A.; Mason, T. O.; Hagerman, M. E.; Poeppelmeier, K. R. In *Chemistry of Advanced Materials: An Overview*; Interrante, L. V., Hampden-Smith, M. J., Eds.; Wiley-VCH: New York, 1998; pp 449−498.

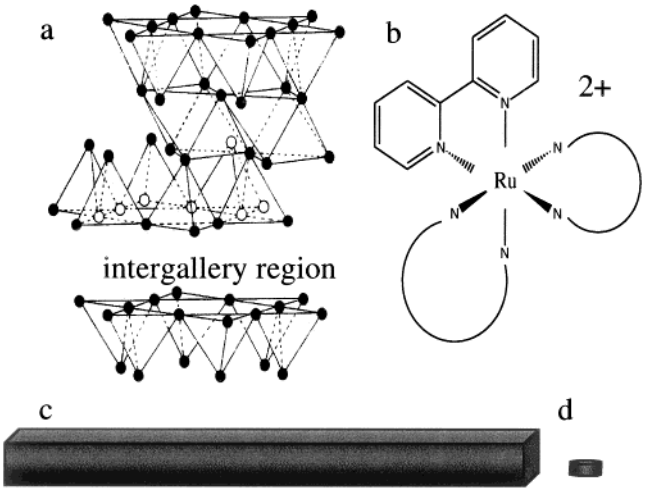

Figure 1. Schematic representations of (a) clay host structure, (b) Rubpy guest structure, (c) hectorite host tactoid, and (d) Laponite host tactoid (shown relative in size to (c)).

%CEC). The films were covered and allowed to exchange over the course of 14 days until complete quantitative adsorption of Rubpy was achieved. The quantitative adsorption was confirmed by the visible absorption spectra of the supernatants where the MLCT band of $[Ru(bpy)_3]^{2+}$ at 452 nm had completely disappeared. In both fabrication methods, films were allowed to dry completely under ambient conditions before characterization.

Characterization. The emission and excitation spectra of the composite films were measured using a PTI Quantamaster Fluorometer. Excitation spectra were collected by monitoring emission traces at 610 nm; phosphorescence spectra were obtained using 468 nm excitation. As there was no observable shift in the excitation maxima upon increased Rubpy loading, 468 nm excitation was used for all films. All measurements were made at room temperature with emission and excitation slit widths of 2 nm. The photomultiplier tube operated at a voltage of 1000 V and the lamp at a power of 75 W. Films were excited in a front-face arrangement at a 45° angle to the incident radiation. Luminescence lifetimes were measured on films at room temperature using a fluorescence lifetime system (Photon Technology LS-100). The excitation source was the 337 nm line of a triggered N_2 lamp. All decay curves were fitted with a double-exponential model. Visible absorption studies were completed with a HP 8453 spectrophotometer. X-ray powder diffraction studies were completed with a Phillips Compact X-ray Diffractometer System (PW1840) operating at a voltage of 45 keV and a current of 35 mA. Fe filtered Co K_α radiation was used with a wavelength of 1.790 Å. All XRD patterns were completed using a step size of 0.010° (2θ) at 2.00 s per step and a receiving slit of 0.3 mm.

Results and Discussion

Host Tactoid Architecture /Guest Microenvironments. Smectite clays offer unique hosts for intercalation compounds.[60−62] In particular, the iron content in hectorite and Laponite is low compared to montmorillonite; this is crucial because iron has been shown to significantly quench $[Ru(bpy)_3]^{2+}$ emission.[35,36,55] We have had much success in casting free-standing films once the Na^+ ions have been exchanged with other cations such as VO^{2+}, Fe^{3+}, Cu^{2+}, and Zn^{2+}.[61] Hectorite and Laponite are layered smectite-type clays; their architectures consists of a 2:1 ratio of tetrahedral to octahedral oxide layers and an intergallery region (see Figure 1). The tetrahedral sheets are comprised of Si^{4+} cations and tetrahedrally coordinated oxide anions that

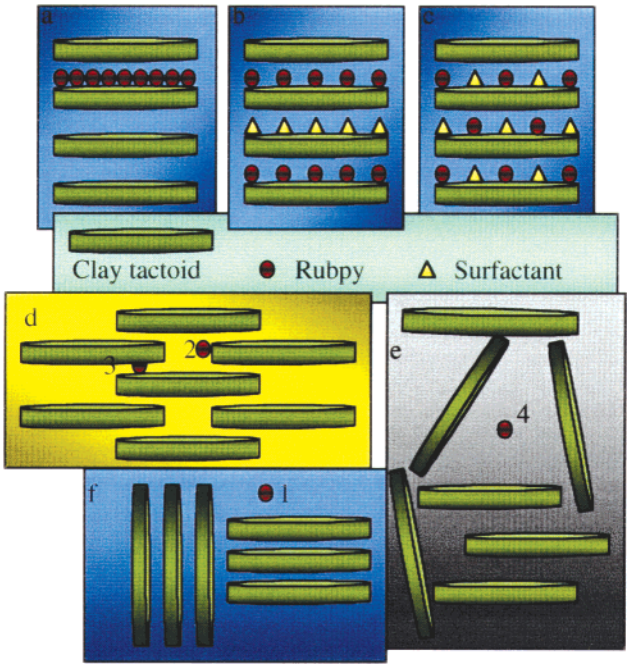

Figure 2. Schematic representations of (a) ion clustering, (b) ion segregation, (c) uniform ion distribution, (d) lamellar ordered tactoids (film), (e) house of cards structure (gel), and (f) tactoid aggregation (powder). Guest microenvironments include the following: (1) surface, (2) edge, (3) intercalated, and (4) micropore. Note that the tactoid shown is for Laponite, and relative sizes of host and guest are not shown to exact scale.

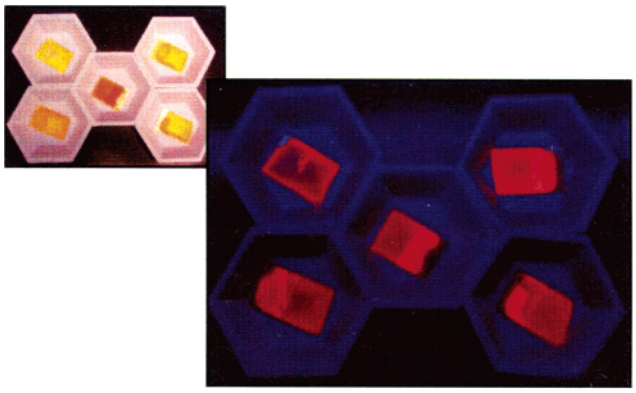

Figure 3. $[Ru(bpy)_3]^{2+}$/zinc Laponite films (top left) and the same films exposed to an ultraviolet light source (bottom right).

share vertexes with the octahedral cations, Mg^{2+} and Li^+. During crystallization, the clay develops a net negative charge owing to substitution of Li^+ on Mg^{2+} sites. The intergallery region exists between repeating tetrahedral−octahedral−tetrahedral (TOT) layers; this region contains water and intergallery cations such as Na^+ that balance the excess negative charge between layers. An important feature of these layered hosts is that their intergallery regions are expandable; their dimensions can adapt to the shape of the guest molecule.[59] In addition, the properties of the host lattice can be tailored by ion exchange of the intergallery cations. Facile ion exchange of zinc by the guest chromophore, Rubpy (see Figure 1b for guest structure), offers efficient routes to photofunctional supramolecular assemblies.

As noted previously, the stacking patterns of the host tactoids (clay platelets or microcrystals) influence guest

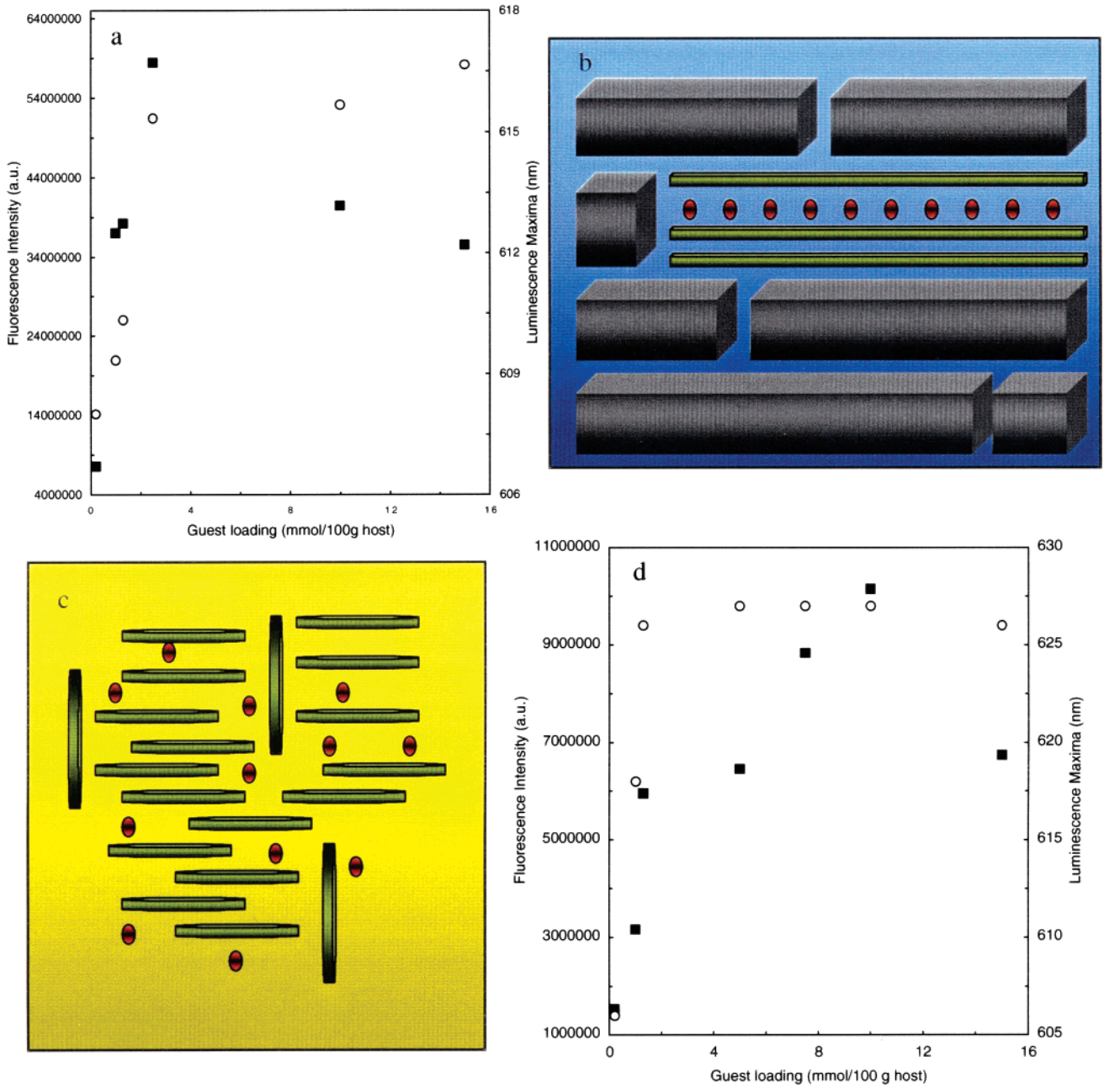

Figure 4. (a) Relative luminescence intensity (■) and luminescence maxima (○) of the LMCT band of the adsorbed $[Ru(bpy)_3]^{2+}$ complexes versus the content of Rubpy incorporated into zinc hectorite films. (b) Schematic of tactoid architecture for Rubpy/Zn hect film. (c) Schematic of tactoid architecture for Rubpy/Zn lap film. (d) Relative luminescence intensity (■) and luminescence maxima (○) of the LMCT band of the adsorbed $[Ru(bpy)_3]^{2+}$ complexes versus the content of Rubpy incorporated into zinc Laponite films.

luminescence through direct mediation of ion clustering and self-quenching phenomena. Figure 2a−c depicts guest intercalation within host lattices showing ion clustering, ion segregation, and uniform ion distribution within the lamellar phase space of the host. These guest arrangements are influenced by specific tactoid architectures depicted in Figure 2d−f. Internal and external microenvironments exist for guest inclusion; the rigidity of these microenvironments is a consequence of clay platelet stacking. After film fabrication, these complexes can be found (1) bound to the surface, (2) intercalated within the intergallery space, (3) bound at tactoid edges, and (4) trapped in micropore regions between tactoids.

Laponite is commercially synthesized through sol−gel methods.[63] Laponite and hectorite are structurally and chemically similar but differ in layer lattice charge, microcrystallite size, and tactoid architecture. Laponite and hectorite exhibit marked differences in tactoid stacking patterns and 2D ordering owing to the differences in the size of their respective microcrystals (see Figure 1c,d). Laponite tactoids are disk-shaped and when monodispersed in water or within film assemblies comprise a single TOT layer. Each individual tactoid is approximately 250 Å in diameter and 10 Å in height. As a result of its small tactoid size, Laponite has a high charge to surface area ratio and can form gel-like matrixes with a "house of cards" structure (see Figure 2e). Hectorite has a brick-shaped structure with a much larger tactoid size (10 000 Å × 1000 Å × 100 Å). Individual hectorite tactoids therefore consist of ap-

proximately three to seven TOT layers.[64] In contrast to the house of cards structure exhibited by Laponite gels, hectorite films show a high degree of lamellar ordering (as shown in Figure 2d).

Luminescence Shifts and Self-Quenching. Rubpy exchanged Zn−Laponite films showed intense luminescence under ambient conditions (Figure 3). The excited-state luminescence of $[Ru(bpy)_3]^{2+}$ has been assigned to the metal-to-ligand charge-transfer (MLCT) state. Incorporation in film assemblies has pronounced influence on the MLCT band. All films studied exhibited optimal luminescence with an excitation wavelength of 468 nm. This is red shifted from the value in aqueous solution. However, there was no observable change in this excitation wavelength upon increased Rubpy loading. This result indicates that in these systems, the surrounding microenvironment only affects the relaxation of the MLCT excited state. Note that the charge-transfer transitions discussed herein are MLCT transitions in absorption but LMCT transitions in emission.

Figure 4 provides information on the relative luminescence intensity and LMCT band luminescence maxima for Rubpy exchanged hectorite and Laponite films with varied guest loadings. The relative luminescence intensities show clear evidence of excited state quenching upon increased guest loading and provide further evidence of previously reported ion clustering.[55] Laponite reaches its maximum luminescence intensity at 10 mmol Rubpy/100 g host (approximately 28% of the CEC), while the hectorite system reaches peak intensity at only 2.5 mmol/100 g host (approximately 5% of the CEC). This variance in optimal loading values may be a consequence of the differences in ion clustering that are mediated by clay tactoid stacking patterns within these films.

Rubpy intercalation within the intergallery region of a single hectorite tactoid (comprised of three stacked or staged platelets) is shown in the green region of Figure 4b. In this model, the tiling of hectorite tactoids is comprised of lamellar ordered clay platelets shown with translation defects.[64] This stacking pattern is clearly more rigid than that of the Laponite system. In the Rubpy/Laponite film, the extent of two-dimensional tiling is less apparent, and the tactoid architecture rests between the stacking patterns shown in Figure 2 (parts d (lamellar ordered film) and e (house of cards gel)). This tactoid arrangement affords a more fluid microenvironment with less extended entrapment of guest chromophores leading to differences in observed photophysical behavior of the included guest.

As previously reported in related $[Ru(bpy)_3]^{2+}$ exchanged hectorite assemblies,[40−45] in these systems Rubpy undergoes self-quenching even at low loading levels (less than 10% of the cation exchange capacity). The mechanism of excited state quenching has been widely researched in these and related systems.[2,3,24,27−29,31,34,36,37,40,47,55,58,65] DeWilde and co-workers[19] have proposed that as the $[Ru(bpy)_3]^{2+}$ molecules get closer together with increased concentration, resonance transfer of excitation energy from one molecule to another occurs leading to loss of emission intensity. Ogawa and co-workers reported significant loss of luminescent intensity when Rubpy centers were confined to a distance of less than 6 nm.[34] Given the low loading levels of our films, ion clustering is the most plausible explanation for the observed quenching behavior.

Table 1. Luminescence Lifetimes and Relative Ratios of Fast (τ_1) and Slow (τ_2) Components Observed for Rubpy Exchanged Hectorite (hect) and Laponite (lap) Films

guest loading (mmol/100 g host)	τ_1(ns)	Q_1(%)	τ_2(ns)	Q_2(%)
1.3 hect	61	16	1116	84
2.5 hect	56	16	538	84
7.5 lap	102	37	557	63
10 lap	80	28	377	72
12.5 lap	47	38	318	62
15 lap	41	27	266	73

Figure 4a,d shows an initial blue shift in luminescence maxima compared to $[Ru(bpy)_3]^{2+}$ in aqueous solution (610 nm) and a subsequent red shift upon increased guest loading. Shifts in the LMCT band reflect changes in the microenvironment of the guest complex and afford intriguing studies of guest−guest and guest−host interactions. Wheeler and Thomas[66] observed similar blue shifts for $[Ru(bpy)_3]^{2+}$ adsorbed on colloidal silica. They concluded that the blue shift was the result of a rigid microenvironment around the guest complex, which prevented excited-state relaxation thus increasing the energy of the LMCT band. Red shifts in these clay systems have been attributed to both guest−guest[26,55] and host−guest[48,67] interactions. Ghosh and Bard[55] attributed spectral red shift to high local concentration of guest species resulting in a hydrocarbon-like environment provided through interactions of the complex with the bpy ligands of neighboring complexes. Endo et al.[67] have observed spectral red shifts for xanthene dyes intercalated in saponite assemblies and attributed the cause of the shift to be a consequence of strong electrostatic interactions between the dyes in their excited states and the negatively charged aluminosilicate clay layers. Partial oxidation of the Ru(II) centers[58] and distortion of the ligands owing to steric constraints[35,46] have also been used to explain the origin of the observed red shift upon adsorption in smectites.

By examining the luminescence maxima data in Figure 4a,d, there is clearly a more pronounced red shift of the Rubpy luminescence maxima in the Laponite system (maximum of 627 nm versus 617 nm for hectorite system). This can be explained if one contrasts the respective tactoid architectures shown in Figure 4b,c. The Laponite microenvironment is more fluid and the water molecules are less rigidly bound to the silicate framework. As a result, it is easier for the solvent molecules to reorient after excitation and solvate the polar MLCT excited state. The complex then emits light from this relaxed excited state yielding the observed red shifted emission. In a rigid matrix, such as the lamellar space of hectorite depicted in Figure 4b, solvent rearrangement is limited by direct interactions with the host framework and spectral red shift is not as pronounced.

(63) *Laponite: The Technical Directory*; Laporte Industries Ltd.: Cheshire, UK, 1999.
(64) Annabi-Bergaya, F.; Estrade-Szwarckopf, H.; Van Damme, H. *J. Phys. Chem.* **1996**, *100*, 4120−4126.
(65) Ogawa, M.; Inagaki, M.; Kodama, N.; Kuroda, K.; Kato, C. *J. Phys. Chem.* **1993**, *97*, 3819−3823.
(66) Wheeler, J.; Thomas, J. K. *J. Phys. Chem.* **1982**, *86*, 4540.
(67) Endo, T.; Nakada, N.; Sato, T.; Shimada, M. *J. Phys. Chem. Solids* **1988**, *49*, 1423−1428.

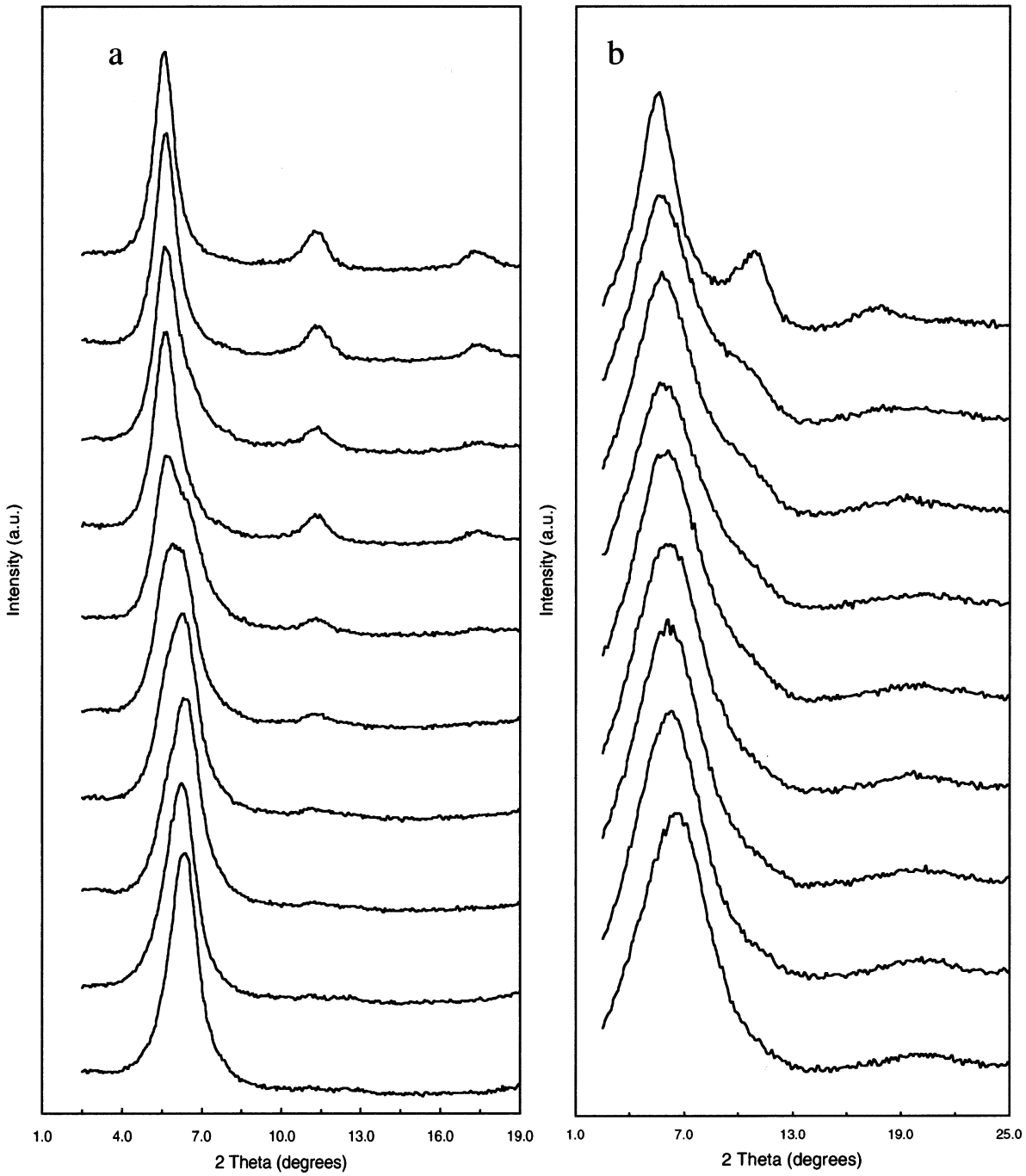

Figure 5. Powder XRD patterns of (a) Rubpy/Zn hect films cast on fused quartz and (b) Rubpy/Zn lap films cast on fused quartz. Rubpy guest loading increases from the bottom to the top of the stacked series.

Luminescence Lifetimes. Luminescence lifetimes of Rubpy/Laponite and Rubpy/hectorite films were measured at room temperature, and lifetime data are summarized in Table 1. Luminescence decay curves were fitted by a double exponential model expressed as

$$I(t) = A_1 \exp(-k_1 t) + A_2 \exp(-k_2 t)$$

where $I(t)$ is luminescence intensity at time t, A_1 and A_2 are preexponential factors, and k_1 and k_2 are decay rate constants. The decay matched a bimodal distribution indicating two distinct microenvironments with a major, slow component and a minor, fast component. Data were only fittable for films with optimized luminescence intensities. In both host systems, luminescence lifetimes increased with decreased guest loadings suggesting lower probability of self-quenching and ion clustering. Note that the minor component is more heavily populated in Laponite, again indicating probable differences in the tactoid architecture and rigidity of guest microenvironments. Higher percentages of the fast component in the Laponite system (even at high loading) are consistent with the assumption of a more fluid Rubpy microenvironment. Differences in Q_1 and Q_2 may also indicate differences in the available microenvironments. That is, while it has been assumed that Rubpy only accesses two microenvironments in hectorite (one internal and one external), Laponite may supply alternative microenvironments including micropore spaces between tactoids (see Figure 2e).

While direct comparison of lifetimes at exactly the same guest loading was not possible owing to low intensities in the hectorite system, it is evident that the projected lifetimes in Laponite are indeed longer compared to hectorite for the same guest loading. An increase in lifetime can be attributed to a decrease in the ν(O−H) modes as energy acceptors for nonradiative decay of the MLCT excited states.[68] In the Laponite system, the free mobility of Rubpy mediated by the differences in tactoid stacking shown in Figure 4b,c leads to minimized interaction with surface hydroxyls and extended luminescence lifetimes.

XRD and Surfactant Studies. Powder XRD patterns were collected to investigate the extent of intercalation of $[Ru(bpy)_3]^{2+}$ into the Zn-hectorite and Laponite host lattices. Only (00*l*) reflections are observed in the XRD pattern of the smectite films owing to their quasi-crystalline layered structures. Figure 5a shows the intense (001) peak with a basal spacing of 13.5 Å. This peak, not present in the Na hectorite powder starting material, is clear evidence of the lamellar structure of the host film. Powder XRD patterns for Rubpy/Zn-hectorite composites with varying guest loading are shown in Figure 5a. As guest loading increases, there is clear evidence of intercalation with the emergence of a sharp, intense peak with a final basal spacing of 19.1 Å. New (002) and (003) peaks at 11.0° 2θ and 17.2° 2θ, respectively, emerge at higher guest loadings and are a direct consequence of Rubpy insertion within the intergallery region of the host framework.

In the Rubpy/Laponite films shown in Figure 5b, a similar trend is observed with an increase from 15.5 to 19.3 Å. New peaks (not present in the unexchanged film) for (002) and (003) reflections at 10.2° 2θ and 18.6° 2θ, respectively, also provide evidence for Rubpy intercalation within the Laponite films. There is clear evidence of preferred orientation of clay platelets in both systems, but the 2D ordering in the hectorite system is more pronounced. The XRD patterns support the tactoid stacking architectures discussed previously and shown in Figure 4.

The interlayer spacing (gallery height) of the $[Ru(bpy)_3]^{2+}$/zinc hectorite intercalation compound was estimated to be 9.5 Å by subtracting the thickness of the TOT layer (9.6 Å)[54] from the observed basal spacing (19.1 Å). Approximately 8.0 Å[43] of this 9.5 Å gallery is filled by the tris(bpy) chelate complex which results in a difference of 1.5 Å. Using a model in which a water molecule occupies 1.1 Å, the remaining 1.5 Å difference may include rigid water molecules hydrogen bonded to the silicate lattice within the intergallery space. Using EPR, powder XRD, and adsorption gravimetry, Annabi-Bergaya and co-workers have proposed similar clay platelet stacking models in a related copper(II) hectorite system.[64] They concluded that a significant amount of water was found both outside and inside the interlamellar space. In a related Rubpy/magadiite study by Ogawa and Takizawa, interlamellar water is also proposed to account for the observed basal spacings.[33] These water molecules mediate host−guest interactions and thus may influence the photophysical properties of the guest.

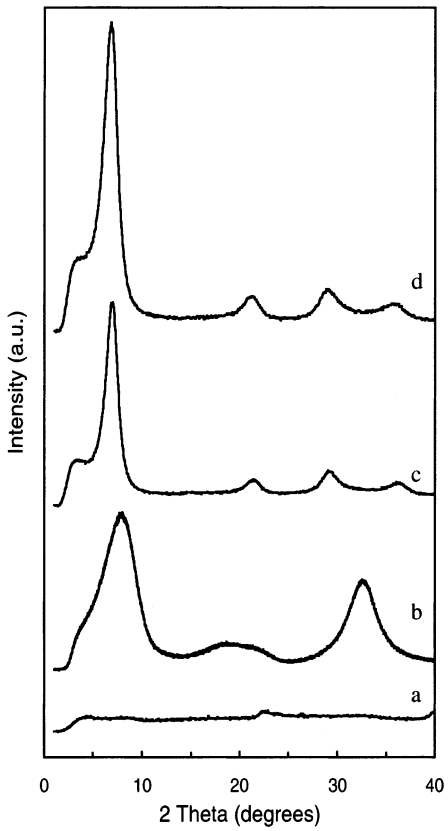

Figure 6. Powder XRD patterns of (a) sodium Laponite powder, (b) zinc Laponite film cast on fused quartz, (c) triethylhexylammonium (TEHA) OML film on quartz, and (d) trimethyldoecylammonium (TMDA) OML film on quartz. Surfactants were exchanged at 100% of the CEC.

Figure 6 provides powder XRD data for Laponite powder, a zinc exchanged Laponite film, and OML films. Laponite powder produces an amorphous XRD pattern (6a), while the zinc Laponite film shows a greater degree of ordering. We have synthesized several organically modified Laponite (OML) films and have explored tactoid tiling using Rubpy as a photoprobe of the inner architecture of the host matrix. With the introduction of surfactants into the Laponite films (TEHA and TMDA OLS films), we see an even greater degree of lamellar ordering with notable Bragg diffraction peaks associated with the (00*l*) family of reflections and an obvious sharpening of the (001) reflection.

At least two models are possible to account for the origin of the peaks at approximately 5° 2θ. The first model involves staging effects (stacking of multiple tactoids to form microcrystalline arrays of two and three stacked tactoids, see Figure 2f). Light scattering studies have confirmed tactoid aggregates in Laponite powder systems.[69] However, this model is unlikely in our systems as Rubpy insertion within these microcrystals would lead to multiple reflections not seen in the XRD data. Note that the competing (00*1*) reflection is not evident in the Rubpy Laponite system without surfactant (Figure 5b). A second and more likely model involves consideration of possible clay/surfactant architectures. These surfactant packing patterns within layered silicates have been studied previously in detail

(68) Innocenzi, P.; Kozuka, H.; Yoko, T. *J. Phys. Chem. B* **1997**, *101*, 2285−2291.

(69) Yan, E. C. Y.; Eisenthal, K. B. *J. Phys. Chem. B* **1999**, *103*, 6056−6060.

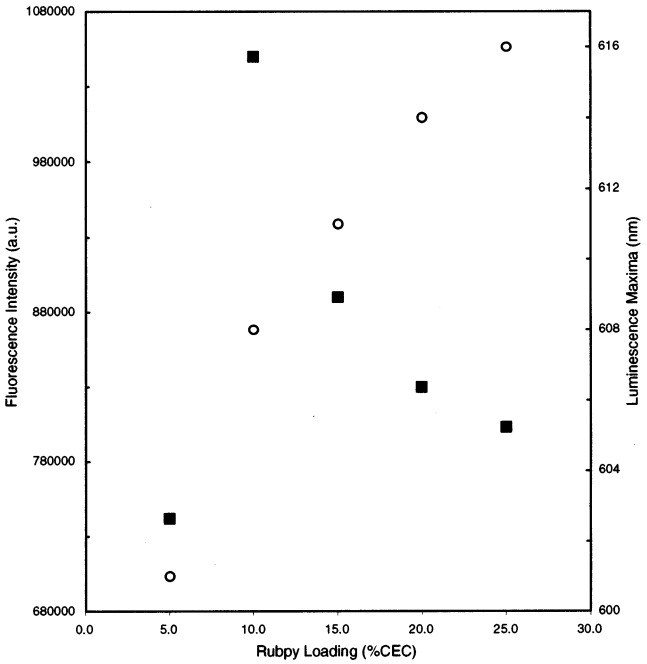

Figure 7. Relative luminescence intensity (■) and luminescence maxima (○) of the LMCT band of the adsorbed $[Ru(bpy)_3]^{2+}$ complexes versus the content of $[Ru(bpy)_3]^{2+}$ incorporated into 50% exchanged trimethylcetylammonium (TMCA) OML films.

by Vaia and co-workers.[51] The primary phase of the Rubpy OML material is most likely comprised of lateral monolayers of surfactacts packed between individually dispersed Laponite tactoids or TOT layers. A secondary phase with paraffin bilayer type packing of surfactant clay assemblies may account for the competing (00*l)* reflection.

Surfactants inhibit the Coulombic attraction between adjacent tactoids (positive edge interfaces with negative oxide surfaces) and cause a breakdown of the house of cards structure by inhibiting tactoid edge/surface interactions. This model is supported by a less pronounced red shift in the luminescence maxima upon increased loading (Figure 7). Emission wavelengths track the data of the more ordered hectorite tactoids (see Figure 4a); this result again indicates a more rigid microenvironment. The more gradual increase in the luminescence maxima upon increased loading indicates a more uniform ion distribution (see Figure 2c) and some control over the extent of ion clustering within these systems. To maintain film quality, surfactant loading must be at or below 50% of the CEC. These successes in 2D ordering of Laponite microcrystals combined with the excellent optical transparency of this host reflect great promise for selective control of chromophore packing for future optoelectronic applications.

Conclusions

Host tactoid architecture influences guest ion clustering and self-quenching phenomena. Rubpy/Laponite films exhibit high potential for optoelectronic and sensor applications owing to excellent optical transparency and intense luminescence. We observed spectral red shift of emission wavelengths upon increased guest loading; the extent of shift in the Rubpy/Laponite system coupled with longer luminescence lifetimes indicate a more fluid guest microenvironment. Luminescence lifetimes increase with decreased guest loadings suggesting decreased probability of self-quenching and ion clustering. Surfactants promote 2D ordering of Laponite tactoids and assist in the prevention of ion clustering. The realization of film composites with enhanced emission traces from zinc hectorite exchanged $[Ru(bpy)_3]^{2+}$ is a logical first step toward the production of optoelectronic devices based on these assemblies. To use $[Ru(bpy)_3]^{2+}$ as a luminescence probe in clay/polymer systems, it is essential to maintain low guest loading. Future work including comparative studies with fluorohectorite and advanced characterization including fluorescence anisotropy, grazing angle XRD, TGA, and oxygen sensing studies are under investigation.

Acknowledgment. The authors would like to thank the Camille and Henry Dreyfus Foundation for their support of this project through a Supplemental Award of the Scholar/Fellow Program (SL-97-010) to M. E. Hagerman. We would also like to thank M. Eastman, T. Porter, M. Kostuk, C. McManaman, and J. Shames for insightful discussions; David McClemens for his generous alumni research summer stipend to S. J. Salamone; K. Hollocher for assistance with powder XRD measurements; and M. K. Carroll and T. C. Werner for support with fluorescence studies.

CM0209160